

# Rheological properties and hydration of ternary cements containing clay brick, clay tile, marble, and phosphogypsum waste

*Propriedades reológicas e hidratação de cimentos ternários contendo resíduos de mármore, porcelanato, bloco cerâmico e fosfogesso*

Ana Rita Damasceno Costa   
Jardel Pereira Gonçalves 

## Abstract

**N**o research demonstrates the effect of combined waste raw materials as an alternative to natural sources in Limestone Calcined Clay Cement (LC<sup>3</sup>). In this context, this study aimed to evaluate the influence of the composition of ternary cements (TCs) containing industrial waste on their rheological and hydration properties. As raw materials, Portland cement and clay brick (CBW), clay tile (CTW), marble (MW), and phosphogypsum (PG) wastes were used. The rheological behaviour of the pastes was analysed by the mini-slump evolution over time and rotational rheometry. Hydration was evaluated by isothermal calorimetry and XRD/Rietveld. An increase in the specific surface area enhances the yield stress and plastic viscosity of the paste. CBW and CTW have pozzolanic reactivity, presenting an increase in the content of non-crystalline phases, including calcium silicate hydrate (C-S-H). The TCs reached at least 70% of the compressive strength of the High Early Strength Portland cement paste. The results suggest that CBW, CTW, MW and PG can be used as an alternative to reduce the clinker factor and decrease the environmental and economic impacts associated with extracting natural raw materials for cement production.

**Keywords:** Ternary cements. Rheology. Hydration. Marble waste. Clay brick waste. Clay tile waste. Phosphogypsum.

## Resumo

*Não há pesquisas que demonstrem o efeito de matérias-primas residuais combinadas como alternativa às fontes naturais em cimentos do tipo LC<sup>3</sup>. Nesse contexto, o objetivo deste estudo é avaliar a influência da composição de cimentos ternários contendo resíduos industriais sobre as suas propriedades reológicas e de hidratação. Como matérias-primas foram utilizados cimento Portland (CP), resíduos de bloco cerâmico (RBC), de porcelanato (RP), de mármore (RM) e fosfogesso (FG). O comportamento reológico das pastas foi analisado pela evolução do mini-abatimento no tempo e reometria rotacional. A hidratação foi avaliada por calorimetria isotérmica e DRX/Rietveld. Um incremento na área superficial específica implicou no aumento da tensão de escoamento e viscosidade plástica da pasta. O RBC e RP possuem reatividade pozzolânica, apresentando incremento do teor de fases não cristalinas (incluindo C-S-H). Os CTs atingiram no mínimo 70% da resistência à compressão da pasta de CP VARI. Os resultados sugerem que os resíduos RBC, RP, RM e FG podem ser utilizados como alternativa para redução do fator clínquer e redução dos impactos ambientais e econômicos associados à extração de matérias-primas naturais para produção de cimentos.*

**Palavras-chave:** Cimentos ternários. Reologia. Hidratação. Resíduo de mármore. Resíduo de bloco cerâmico. Resíduo de porcelanato. Fosfogesso.

<sup>1</sup>Ana Rita Damasceno Costa  
<sup>1</sup>Universidade Federal da Bahia  
Salvador - BA - Brasil

<sup>2</sup>Jardel Pereira Gonçalves  
<sup>2</sup>Universidade Federal da Bahia  
Salvador - BA - Brasil

Recebido em 15/11/21  
Aceito em 12/04/22

## Introduction

Incorporating supplementary materials in alternative cements has a significant impact on the fluidity of their pastes, often changing the water demand to achieve workability similar to that of blends with ordinary Portland cement (PC) (ZHANG *et al.*, 2012). The workability of LC ternary cements (TCs) is governed by calcined clay, which retains water, reducing the effective interaction between water and the binder. The use of limestone containing minute amounts of organic components alters the rheological properties of the system (BESSAIRES-BEY *et al.*, 2016; FAVIER *et al.*, 2018; LI *et al.*, 2021). Ferreiro, Herfort and Damtoft (2018) found that clays with a  $\text{SiO}_2:\text{Al}_2\text{O}_3$  molar ratio equivalent to 1:1 increase the water demand in the TCs compared to those with a 2:1 ratio to achieve the same consistency index. By fixing the water/cement ratio, clays of the 1:1 type may require up to three times more superplasticizer admixture.

Intervening factors such as the high specific surface area and layered structure of clay minerals, as well as the high concentration of sulfate ions and their implications for the workability of the pastes were only superimposed after developing advanced superplasticizers, modifying the structure of polymer admixtures, as developed by Akhlaghi *et al.* (2017). However, this alternative has been rarely explored and is not commercially available. Previous studies have verified a reduction in the workability of TC pastes compared to ordinary PC, but qualitatively. Using techniques, such as rotational rheometry and mini-slump evolution over time can quantitatively assess the impact of TC dosage on the rheological properties of pastes and correlate its parameters with other aspects, such as hydration, mechanical properties, or durability.

The mineralogical composition of TC pastes influences their rheological properties and fundamentally depends on the clay reactivity, substitution content, cement composition, and age (TIRONI *et al.*, 2014a). The effect of partial PC replacement by highly reactive calcined clays on hydration is a combination of a filler effect, increasing the degree of hydration at early ages and the pozzolanic reaction of calcined clays at more advanced ages (ALUJAS *et al.*, 2015). Calcined clays favor the formation of hemi and monocarboaluminate-type phases and influence the microstructure of hydration products, increasing the length of the C–A–S–H chain where aluminum replaces silicon (ALUJAS *et al.*, 2015; PUERTA-FALLA *et al.*, 2015). However, no studies demonstrate the effect of waste raw materials as an alternative to natural sources in ternary systems such as LC<sup>3</sup>.

Considering the environmental impacts of extracting and using natural raw materials for cement production, the present study is relevant because it aims to add value to the waste materials used and reduce their deposition in sanitary landfills. Phosphogypsum is a waste material from the production of phosphoric acid in the fertiliser industry, and its main chemical composition is  $\text{CaSO}_4 \cdot 2\text{H}_2\text{O}$  (RASHAD, 2017). Its potential for use as a set retarder has been demonstrated in previous research on ordinary PC (ALTUN; SERT, 2004; ROSALES *et al.*, 2020), magnesium phosphate cement (HAQUE *et al.*, 2020), and ternary cement (COSTA *et al.*, 2021). However, in this last approach, the evaluation of the rheological properties was not carried out.

Thus, the present study aimed to evaluate the influence of the composition of ternary cements containing waste on their rheological and hydration properties. To do this, ternary samples were produced containing PC, clay tile waste (CTW) or clay brick waste (CBW), marble waste (MW), and phosphogypsum (PG). The analysis focuses on the variation of both the calcined clay source (CTW or CBW) and the utilisation of different ceramic waste/marble waste ratios.

## Materials and methods

### Materials

The raw materials used in this study were a Brazilian High Early Strength Portland cement (type CP-V-ARI), quartz (Q), phosphogypsum (PG) and marble waste (MW), clay brick waste (CBW), and clay tile waste (CTW). High early strength Portland cement (PC) was applied as a source of clinker for the ternary cements (TC). In PC, the clinker content plus calcium sulfate constitutes 90 to 100% of the material and the complementary fraction is carbonate material, according to the NBR 16697: Portland cement specification: requirements (ABNT, 2018). Thus, PC was chosen because it has the highest clinker content among the cements available in the regional market and because it has calcium carbonate as an addition, a mineral that constitutes the TCs developed in this research. The CBW was discarded material from a red ceramic brick factory in the city of Alagoinhas, Bahia. The CTW was waste material from a floor covering distributor in the city of Salvador, Bahia. The sample was from a single batch and an enamelled tile model. The MW was of Bege Bahia type, a by-product obtained from a company that cuts and manufactures ornamental pieces in Salvador. Phosphogypsum was waste from phosphoric acid production in a fertiliser industry in Uberaba, Minas Gerais.

The CBW, CTW, and MW waste consisted of pieces up to 10 cm in length and were initially ground in an I 4198 jaw crusher (Pavitest). These by-products and the PG were dried in an oven at 35 °C for 24 h. The fraction passing through a standard 1.18 mm sieve was then milled in a PM 100 (Retsch) planetary ball mill equipped with a 500 cm<sup>3</sup> stainless steel milling jar. Moreover, 1600 spheres (stainless steel,  $\phi$  5 mm) were used and the volume of each material was set at 75 cm<sup>3</sup>. That is, 210 g CBW, 195 g CTW, 208 g MW or 183 g PG. PG and MW were milled at a rotation speed of 300 rpm for 5 and 20 min, respectively. The CBW and CTW were milled at a speed of 400 rpm for 15 and 30 min, respectively. Moreover, 0.2% propylene glycol dispersant was used to mitigate the agglomeration of CBW and CTW in the spheres and against the inner faces of the milling jar. To mill the MW and PG, 0.4% of the dispersant was used. The physical properties of the raw materials are shown in Table 1.

The specific mass was determined by a helium gas pycnometer using a Micromeritics AccuPyc II 1340 analyser. The specific surface area was calculated by the Brunauer-Emmett-Teller (BET) method by applying nitrogen physisorption isotherms at -196 °C in the ASAP 2020 equipment (Micromeritics). CBW, MW, and Q were previously degassed under N<sub>2</sub> flow at 300 °C for 1 h and at 4 mmHg. The degassing conditions (N<sub>2</sub> flow at 40 °C for 16 h and 4 mmHg) of the PC and PG were defined to avoid dehydration of CaSO<sub>4</sub>·2H<sub>2</sub>O (MANTELLATO; PALACIOS; FLATT, 2015).

Specific heat was determined using a DSC-50 differential scanning calorimeter (Shimadzu) and following the E 1269-11: standard test method for determining specific heat capacity by differential scanning calorimetry (AMERICAN..., 2018). Particle size distribution was determined by laser diffraction using a Mastersizer 3000 analyser (Malvern Instruments) equipped with an Aero S dry powder disperser.

The ceramic wastes (CBW and CTW) were processed by milling to ensure a similar D<sub>50</sub> diameter between the materials and below that presented by the PC (Table 1). Thus, the effect of changing the particle size can be reduced. In this sense, this study prioritises discussing the particle shape effect, which is indicated by the specific surface area analysis. CBW has a surface area of approximately twice that verified for the CTW and Q. The specific heat was determined to calculate the heat capacity of the pastes. It aims to guarantee the equivalence with this same property in the reference samples on the isothermal calorimetry analysis.

Table 2 presents the chemical composition of the raw materials obtained by X-ray fluorescence spectrometry (XRF) using an S8 Tiger instrument (Bruker). The loss on ignition (LOI) was determined by thermogravimetric analysis (TG) performed on a DTG - 60H thermal analyser (Shimadzu). Approximately 10 mg of the powder samples were analysed in alumina crucibles, according to C 114-18: standard test methods for chemical analysis of hydraulic cement (AMERICAN..., 2018). The heating rate was 10 °C min<sup>-1</sup> from 25 °C to 1000 °C, in a synthetic air atmosphere (20% O<sub>2</sub> and 80% N<sub>2</sub>) and with a flow rate of 50 mL.min<sup>-1</sup>.

Table 1 - Physical properties of raw materials

Property	PC	CBW	CTW	MW	PG	Q
Specific mass (kg m <sup>-3</sup> )	3272	2814	2601	2781	2438	2665
Specific surface area BET (m <sup>2</sup> kg <sup>-1</sup> )	1301	9395	4540	9681	5119	4327
Specific heat (J g <sup>-1</sup> °C <sup>-1</sup> )	1.13	1.10	0.83	1.25	1.08	0.81
D <sub>10</sub> (µm)	1.87	0.77	0.83	0.73	1.37	1.95
D <sub>50</sub> (µm)	11.60	3.14	3.14	3.69	7.98	11.10
D <sub>90</sub> (µm)	34.08	10.20	8.61	15.33	32.05	37.70

Table 2 - Composition of oxide raw materials (%)

Material	CaO	SiO <sub>2</sub>	MgO	SO <sub>3</sub>	Al <sub>2</sub> O <sub>3</sub>	Fe <sub>2</sub> O <sub>3</sub>	K <sub>2</sub> O	TiO <sub>2</sub>	P <sub>2</sub> O <sub>5</sub>	Na <sub>2</sub> O	Others	PG
PC	59.02	15.38	6.38	4.92	3.33	2.97	0.91	0.21	0.11	0.10	0.27	6.40
CBW	0.09	64.79	1.29	0.04	20.86	6.55	3.43	0.94	0.11	0.11	0.67	1.12
CTW	1.29	65.02	0.98	0.03	20.23	4.60	2.16	0.51	0.06	3.06	1.99	0.07
MW	49.03	4.53	3.71	0.04	0.45	0.27	0.07	0.03	0.01	n.d.	0.11	41.75
LOI	33.02	1.10	0.02	40.43	0.11	0.48	49 ppm	0.68	0.73	n.d.	1.09	22.34

Note: LOI: Loss on ignition (1000 °C) determined by thermogravimetric analysis; n.d.: not detected; and ppm: parts per million.

The mineralogical composition of the raw materials was calculated by X-ray diffraction (XRD) combined with quantitative analysis by the Rietveld method using the GSAS II software version 3913 (TOBY; VON DREELE, 2013). The refined parameters were the phase scale factor, background coefficients (Chebyshev polynomial), sample displacement error, unit cell parameters, and instrumental parameters (W, X, V, and U). For phosphogypsum, the March-Dollase preferential orientation coefficient was refined for the gypsum and brushite phases. The samples were analyzed in a D8 Advance diffractometer (Bruker AXS) (radius of 280 mm) with Cu K $\alpha$  radiation ( $\lambda = 0.154$  nm) at 21 °C. The X-ray tube was operated at 40 kV and 40 mA. Data were collected in an angular range from 5° 2 $\theta$  to 70° 2 $\theta$ , with a step of 0.02° and a time per step of 1 s. CBW and CTW have significant levels of amorphous phases (75.31 and 56.18%, respectively). The calcination of natural clay up to 850 °C promotes the dehydroxylation of clay minerals, which in turn causes a structural disorder and results in the formation of amorphous phases (SABIR; WILD; BAI, 2001). In industry, quartz is used as an additive to improve the thermal and dimensional stability of clay bricks and tiles.

XRF analysis identifies the total SiO<sub>2</sub> content in the sample, that is, the percentage of the oxide combined in different minerals regardless of the degree of crystallinity. The XRD/Rietveld, with a correction of the amorphous content, can quantify the crystalline minerals of the material. Applying a stoichiometric analysis of the crystalline phases, the SiO<sub>2</sub> content combined with the crystalline phases can be determined. The difference between this value and the total SiO<sub>2</sub> content identified by XRF provides the SiO<sub>2</sub> content present in the non-crystalline phase of the material. In calcined clay materials, the amorphous fraction largely corresponds to clay minerals after the dehydroxylation step (SABIR; WILD; BAI, 2001). Thus, for CBW, for example, 64.79% of SiO<sub>2</sub> was detected by XRF, and XRD/Rietveld detected 22.35% of quartz. In other words, the SiO<sub>2</sub> content in the clay mineral of this clay waste is 42.44%. As the Al<sub>2</sub>O<sub>3</sub> content is 20.86%, an Al<sub>2</sub>O<sub>3</sub>/SiO<sub>2</sub> ratio of approximately 2.0 is identified, which is associated with the presence of montmorillonite. For CTW, this proportion is 1.8, suggesting the presence of clay minerals in proportions of 1:1 (kaolinite) and 2:1 (montmorillonite). MW contains 70.97% CaCO<sub>3</sub>. The PG has 63.51% of CaSO<sub>4</sub>.2H<sub>2</sub>O.

## Production and curing of ternary cement pastes

The standard composition of LC<sup>3</sup> cement is 50% clinker, 30% calcined clay, 15% limestone, and 5% gypsum (ANTONI *et al.*, 2012; DHANDAPANI; SANTHANAM, 2017; TIRONI; SCIAN; IRASSAR, 2017; MARAGHECHI *et al.*, 2018). The 0.72% calcium sulfate (CaSO<sub>4</sub>) content of the cement (which produces 0.91% gypsum when in contact with water) was corrected to keep the CaSO<sub>4</sub> source content at 5% (RAMACHANDRAN *et al.*, 2002). Thus, 4.64% PG was added as a substitute for natural gypsum. Two ternary cements were produced with the standard dosage (Table 3), replacing the calcined clay by CBW (TC.CBW) and by CTW (TC.CTW).

Two reference samples were produced. The first contains pure PC. In order to evaluate the contribution of the filler effect, a second reference sample (PC.Q) was determined to contain quartz as inert material in the same content as the supplementary cementitious materials (SCM) in the ternary cement (ceramic waste + MW).

The effect of the ceramic waste /MW ratio was analysed for the TCs considering the non-crystalline CaCO<sub>3</sub>/Al<sub>2</sub>O<sub>3</sub> ratio among the raw materials. The mass fractions of CBW or CTW for MW were adjusted so that the molar ratios of Al<sub>2</sub>O<sub>3</sub> and CaCO<sub>3</sub> in the amorphous phase of each material remained equivalent to 1:1. The sample composition was determined using a CaCO<sub>3</sub> content of 70.97% for the MW and a non-crystalline alumina content of the clay waste of 19.83% for the CBW and 10.17% for the CTW. Therefore, the CBW/MW ratio was 3.6 in the first sample (TC.CBW<sub>II</sub>) and the CTW/MW ratio was 7.0 in the second sample (TC.CTW<sub>II</sub>).

Table 3 - Composition of ternary cements and reference samples (%)

Sample	PC	CBW	CTW	MW	Q	PG
TC.CBW	50.36	30.00	-	15.00	-	4.64
TC.CBW <sub>II</sub>	50.36	35.17	-	9.83	-	4.64
TC.CTW	50.36	-	30.00	15.00	-	4.64
TC.CTW <sub>II</sub>	50.36	-	39.36	5.64	-	4.64
PC.Q	50.36	-	-	-	45.00	4.64
PC	100	-	-	-	-	-

Except for isothermal calorimetry, all mixtures consisted of 500 g of anhydrous material with 275 g of deionized water ( $w/c = 0.55$ ). The procedure was carried out in a Hamilton mixer model HMD 200 from Fann. The previously homogenised anhydrous material was added to the water and mixed for two minutes at a speed of 21000 rpm. Then, there was a pause of one minute to loosen the material adhered to the inner faces of the container using a spatula. The paste was then mixed for a further two minutes at a speed of 14000 rpm. The water/solids ratio was fixed in a preliminary study with the ternary compositions to indicate the minimum water content so that the resulting paste would not reach the limiting viscosity of the equipment during rotational rheometry.

For the XRD analysis, the pastes were conditioned in sealed plastic packages until the age of analysis (1, 3, 7, 28, and 91 days) to avoid carbonation of the hydrated products. For the axial compressive strength tests, the samples were moulded into six cubic specimens with a 5 cm edge (for each age) using metallic moulds. Consolidation was performed on a vibrating table, distributing the material into three subsequent layers and applying vibration for 10 seconds in each layer. The samples were demoulded after 24 hours of production, then subjected to submerged curing in tap water without additives and in an environment with a temperature of 20 °C.

### Mini-slump test

The mini-slump test was applied to study the effect of the composition of ternary cements on the rheological properties of the pastes over time. A cone with a lower diameter, upper diameter, and height of 40 mm, 20 mm, and 60 mm, respectively, was filled with the paste, applying 20 strokes with a spatula to remove possible bubbles. The spread diameter was then recorded after removing the cone at 5, 15, and 30 minutes after the first contact of the cement with the water, allowing the evaluation of the opening loss over time. The pastes were manually homogenised for 10 seconds, and the measurement was performed after 15 seconds of the paste in the mini-slump cone, recording the average value of two spread diameters perpendicular to each other.

### Rotational rheometry

In order to comparatively analyse the rheological parameters of the produced ternary cement pastes and reference compositions, tests were carried out on the Chandler Engineering model 3530 viscometer with coaxial cylinders. The test routine and the determination of tension and viscosity parameters were carried out following NBR 9831: oil well cements: specifications and test methods (ABNT, 2020). The load profile consists of pre-shearing the sample to a maximum rotational speed of 600 rpm for 60 seconds, followed by a decrease in rotational speed in steps of 20 seconds to 300, 200, 100, 60, 30, 20, 10, 6, and 3 rpm.

The yield stress and plastic viscosity for each fluid were estimated by applying Bingham models in the descending curves of each shear cycle. The initial and final gel strength data were determined based on the maximum shear stress reached by restarting the paste rotation after resting for 10 seconds and 10 minutes, respectively. Their values represent the resistance of fluid upon restarting the movement, and the difference between the measurements indicates the stability of the yield stresses of the paste over time (ABNT, 2020).

### Isothermal calorimetry

Isothermal calorimetry was performed to evaluate the influence of the composition on the hydration kinetics of TC pastes at 20 °C and during the first 72 h, following the C 1679 guidelines - Standard practice for measuring the hydration kinetics of hydraulic cementitious mixtures using isothermal calorimetry (AMERICAN..., 2017). For this purpose, an eight-channel TAM Air isothermal calorimeter (TA Instruments) was used. According to the mixing proportions in Table 3, 100 g of ternary cement and 55 g of deionized water were mixed in a plastic container for 2 min at 14000 rpm using a mechanical mixer. Approximately 6 g of the sample was transferred to a 20 mL glass ampoule, which was sealed and placed in the instrument. The time between first contact with water and final placement in the calorimeter was minimised to less than 3 minutes. Due to external mixing, an initial delay of 30 min was preset to allow samples to reach the target temperature before starting data collection.

### X-ray diffractometry (XRD) and quantitative analysis by the Rietveld method

XRD was applied to identify the mineralogical composition of TC pastes after 1, 3, 7, 28, and 91 days of hydration. The samples were analysed in a D8 Advance diffractometer (Bruker AXS) (radius of 280 mm) with Cu K $\alpha$  radiation ( $\lambda = 0.154$  nm) at 21 °C. The X-ray tube was operated at 40 kV and 40 mA. After

mixing, the pastes were conditioned in sealed plastic packages until the age of analysis to avoid carbonation of the hydrated products. The samples were then hand pulverised in a porcelain mortar until they all passed through a standard 75  $\mu\text{m}$  aperture sieve. Data were collected in an angular range from  $5^\circ 2\theta$  to  $70^\circ 2\theta$ , with a step of  $0.02^\circ$  and a time per step of 1 s. During the readings, the samples were rotated at 15 rpm around the vertical axis of the goniometer to improve the particle statistics and minimise the preferential orientation effect.

Quantitative analysis was applied using the Rietveld method using the GSAS II software version 3913 (TOBY; VON DREELE, 2013). The identified crystalline phase patterns were obtained as crystallographic information files (CIF) taken from the Inorganic Crystal Structure Database (ICSD). For all XRD standards, the general parameters refined were the phase scale factor, background coefficients (Chebyshev polynomial), sample displacement error, unit cell parameters, and instrumental parameters related to peak shape (W, X, V, and U).

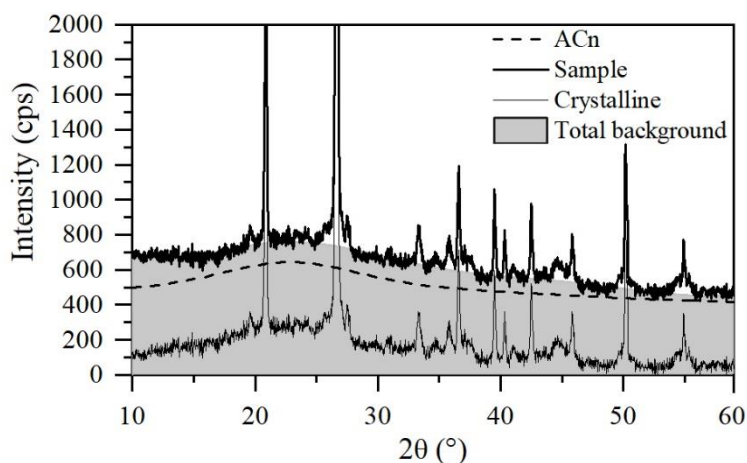
The Rietveld method consists of optimising parameters to obtain the best possible agreement between observed and calculated diffractogram patterns. The refinement result corresponds to the mass fraction of each identified crystalline phase (ARANDA; DE LA TORRE; LEÓN-REINA, 2012). The goodness of fit was evaluated by the chi-square factor ( $X^2$ ), which corresponds to the goodness of fit squared. In GSAS II,  $X^2$  is the sum of squared deviations between observed and calculated values for each data point. Usually, the result is considered reliable if the value of  $X^2$  is in the range of 1.0 to 2.0 (ABU; MOHAMED; AHMAD, 2014).

In this study, the Degree of Crystallinity (DOC) method was used to determine the unquantified amorphous and crystalline content in the samples. This approach consists of estimating the degree of crystallinity by applying the calculation of the areas referring to the crystalline (sharp XRD peaks) and non-crystalline (amorphous halos below the baseline) phases in a diffraction interval (Figure 1) (CALLIGARIS *et al.*, 2018). The detailed development of this methodology is described by Mittemeijer and Scardi (2004). The amorphous (ACn) content was adjusted by a single Pseudo-Voigt peak inserted into the baselines of the diffractograms. It was determined by the ratio between the non-crystalline and total area of the XRD curve, according to Madsen, Scarlett and Kern (2011). The non-crystalline area comprises the area under the Pseudo-Voigt function, while the crystalline area is the complementary fraction.

## Axial compressive strength

The axial compressive strength characteristics were evaluated in pastes in cubic specimens with a 5 cm edge, following the C 109 procedures - Standard Test method for compressive strength of hydraulic cement mortars (AMERICAN..., 2016). Assessments were performed at 1, 3, 7, 28, and 91 days after moulding.

Figure 1 - Section of an XRD pattern indicating the contribution of amorphous (ACn) and crystalline areas calculated according to Mittemeijer and Scardi (2004)



## Results and discussions

### Influence of dosage on the rheological properties of ternary cements

The TC pastes showed greater conservation of spread diameter over time (Figure 2), with a reduced variation ( $\leq 23\%$ ) in spread between the initial measurement and that performed at 30 minutes. This behaviour was even more accentuated in the paste with CTW ( $\leq 9\%$ ). The TC pastes, in general, showed lower spread when compared to the PC, on average 13% lower for the TC.CTW and 28% for the TC.CBW. This effect may be related to the higher specific surface area of the SCM, which can increase the water demand and reduce the fluidity of the paste (LONG *et al.*, 2021). The reduction in spread diameter results from the decrease in the thickness of the paste available to lubricate the SCM particles during the flow of the mixture (MEHDIPOUR; KHAYAT, 2017). The most evident reduction for systems containing CBW corroborates the mineralogical composition analysis and is attributed to the presence of low-grade clays (montmorillonite). Although the clay that came from the CTW also contains montmorillonite, its content is reduced due to the contribution of the surface coating layer of porcelain ( $\text{SiO}_2$ ), implying specific surface area alteration and, therefore, in the spreading of the pastes containing CTW. The reduction in the spread diameter between the PC and TC pastes is in line with the range verified in previous studies (15 to 30%), in which 50% of the clinker was replaced by calcined clay and calcitic limestone (LONG *et al.*, 2021; NAIR *et al.*, 2020).

Performing a weighted average considering the proportions of the materials used and the  $D_{10}$ ,  $D_{50}$  and  $D_{90}$  diameters, the diameters of the particles of the TCs as a whole can be estimated (Table 4). The samples showed similar diameters regardless of the proportion of ceramic waste (CTW or CBW)/MW applied.

Figure 3 presents the rheological parameters obtained by applying the Bingham model to regress the flow curves of each paste. The samples with CBW showed higher yield stresses. This effect can be explained by the high specific surface of the waste (about twice that of the CTW), which increases the amount of water adhering to the grains and reduces the free water that would improve the flow of the mixture. Making a comparison between the dosing methods, it can be observed that the conventional dosing led to higher yield stresses. The reduction of the MW content can explain this performance as it has the highest specific surface area. Regarding the plastic viscosities, the values generally follow the same trend as the yield stresses. The PC.Q sample showed intermediate viscosity to those of PC and TC. This behaviour can be explained by the increase in the total specific surface area when adding quartz, whose property is approximately three times greater than PC and twice that of CBW. According to Mehdipour and Khayat (2017), the surface area is the predominant factor on the rheological parameters of cementitious pastes and is mainly associated with the particle size factor.

The difference between the initial and final gel values indicates the stability of the yield stresses of the paste over time. The TC pastes presented higher values when compared to the PC paste references, showing evidence of the influence of the SCM on the rheological parameters. The initial and final gel strength variations were greater for pastes with CTW.

Figure 2 - Spread diameter of PC and TC pastes over time

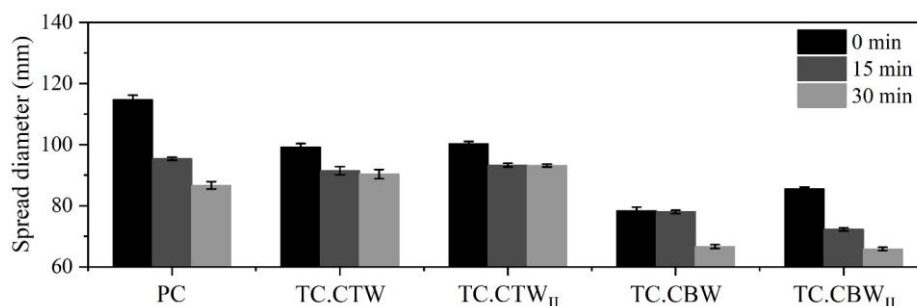
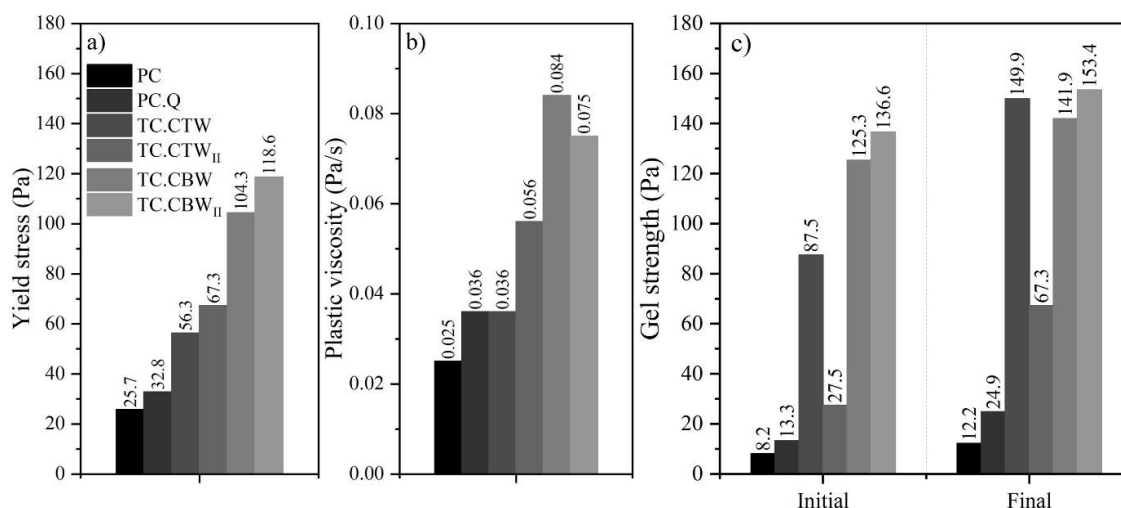


Table 4 - Diameters  $D_{10}$ ,  $D_{50}$  and  $D_{90}$  estimated for ternary cements

Sample	TC.CBW	TC.CBWII	TC.CTW	TC.CTWII
$D_{10}$ ( $\mu\text{m}$ )	1.35	1.35	1.36	1.37
$D_{50}$ ( $\mu\text{m}$ )	7.71	7.68	7.71	7.66
$D_{90}$ ( $\mu\text{m}$ )	24.01	23.74	23.53	22.90

Figure 3 - (a) Yield stress, (b) plastic viscosity and (c) gel strength of reference pastes and TCs



The physical property that determines the rheological properties of pastes is the specific surface area (CLAISSE; LORIMER; OMARI, 2001). An increase in its value results in an increase in the percentage of water adhering to the surface of the grains and a reduction in free water, thus hindering the flow of the mixture. This relationship can be observed in Figure 4. Values for the average specific surface area of the cements were assigned to the pastes. These were calculated according to the weighted average of the individual specific surface areas and the contents of each raw material in the mixture.

The results suggest a direct correlation between the reduction of the spread diameter and the increase in the specific surface area. Due to the physical properties of the raw materials, the pastes with CBW showed lower workability. A correlation between the surface area and yield stress, and plastic viscosity can be observed. The PC reference paste presents the lowest values of yield stress, plastic viscosity, initial gel and final gel. On the other hand, this composition indicated the largest spread diameters. The increment of SCM in the TC pastes increases the specific surface and consequently has the opposite behavior to that of the PC paste. A similar performance was verified by Perez *et al.* (2015), Favier *et al.* (2018), and Ferreiro, Herfort and Damtoft (2018).

### Influence of dosage on ternary cement hydration

During the initial reactions, the TC samples present a higher heat flow when compared to the references (Figure 5). The higher content of  $\text{Ca}^{2+}$  ions from supplementary raw materials may explain this effect. The main hydration peak occurs around 10 hours after the test has started and is attributed to the formation of hydrated calcium silicate, calcium hydroxide, and ettringite. The difference between the heat flow of PC and PC.Q pastes indicates the contribution associated with the filler effect.

The TC samples showed a higher maximum heat flow than the reference, indicating a contribution to the hydration process in addition to the filler effect. It should be considered, however, that the contribution of the paste with CTW was minimal and may be associated with better packing of the cement particles. The increase in the main hydration peak is related to the higher formation of calcium hydroxide (CH), C-S-H, and ettringite, and is higher for CBW, followed by pastes with CTW.

The reduced effect of CTW on the hydration kinetics (compared to CBW) may be associated with the temperature of the heat treatment while producing the materials. Clay calcination generally occurs in the temperature range of 600 and 850 °C. It results in the dehydroxylation of clay minerals, through which an amorphous phase is formed and, therefore, its reactivity is potentiated when incorporated into the cement matrix (HOLLANDERS *et al.*, 2016). When exceeding this temperature range, the recrystallisation processes begin and there is a decrease in the specific surface and the pozzolanic reactivity of the material (TIRONI *et al.*, 2014a). Thus, when comparing the temperatures practiced by the industry in the clay tile production (1150 to 1250 °C) and clay brick (up to 950 °C), the CTW may initiate the recrystallisation process (OLIVEIRA.; HOTZA, 2015; TIRONI *et al.*, 2014b). Thus, the specific surface area of the CTW is reduced, mitigating the contribution of the nucleation effect on the cement hydration kinetics.

The evolution of the accumulated heat is shown in Figure 6. The change in the composition of the SCM differentiates the curves from the initial minutes of hydration. The total heat in the hydration reaction of the

samples with CBW varied slightly between the different dosages of this waste. The data suggest that the alumina: calcium carbonate ratio change did not influence the hydration kinetics between 48 and 72 hours. On the other hand, samples with CTW in 72 hours showed accumulated heat about 10% higher for the TC.CTWII paste. This effect may be associated with the conversion of ettringite into monosulfoaluminate (AFm) in the last hours, as can be seen by a slight peak in the heat flow curve.

The calorimetry analysis indicates that the TC pastes showed a slightly higher formation of C-S-H and ettringite at the main hydration peak. The increase in heat flow was a maximum of 0.5 mW/g of cement, which was attributed to the nucleation effect generated by the presence of smaller particles. Samples with CBW showed a higher hydration rate when compared to CTW. Formulations with the unconventional dosage (TC.CBWII and TC.CTWII) showed a subtle difference (< 1.6%) in the heat data up to 3 days, which was not enough to confirm a contribution beyond that justified by the better packaging of the particles.

The diffractometry data of the reference pastes (PC and PC.Q) with 1, 3, 7, 28, and 91 days are shown in Figure 7. The crystalline fraction of the samples essentially comprises calcium hydroxide, ettringite, quartz, calcite, alpha belite and beta belite (C<sub>2</sub>S α and C<sub>2</sub>S β), alite (C<sub>3</sub>S), and ferrite (C<sub>4</sub>AF). The diffractometry data of the ternary pastes produced with porcelain and marble waste (TC.CTW and TC.CTWII) are shown in Figure 8. The crystalline fraction of the hydrated samples comprises portlandite, ettringite, calcite, quartz, sillimanite, dolomite, alite (C<sub>3</sub>S), and ferrite (C<sub>4</sub>AF). The qualitative analysis of the mineralogical composition of the ternary pastes produced with clay brick and marble waste (TC.CBW and TC.CBWII) is shown in Figure 9. The crystalline fraction of the samples comprises portlandite, ettringite, calcite, quartz, dolomite, mullite, alpha belite and beta belite (C<sub>2</sub>S α and C<sub>2</sub>S β), alite (C<sub>3</sub>S), and ferrite (C<sub>4</sub>AF).

Figure 4 - Correlation between the rheological properties and the specific surface area of reference and ternary cements

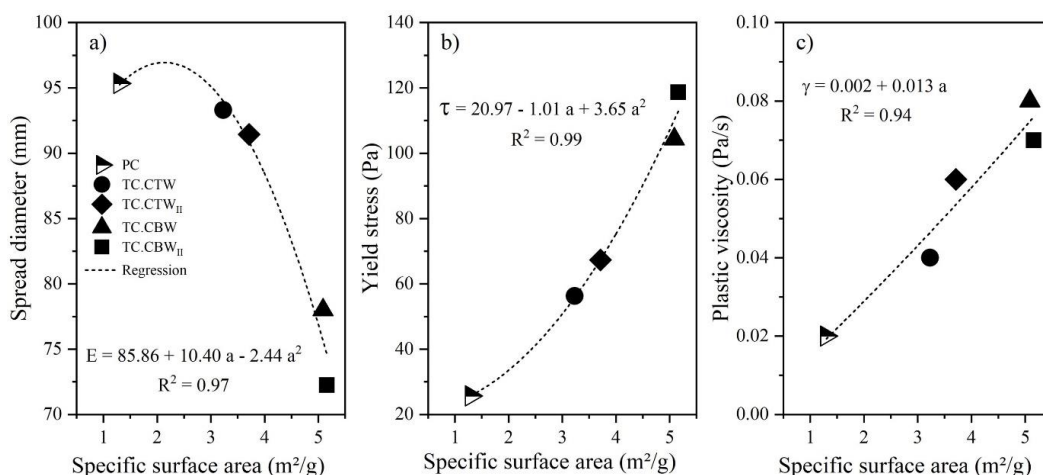


Figure 5 - Evolution of the heat flow during cement hydration

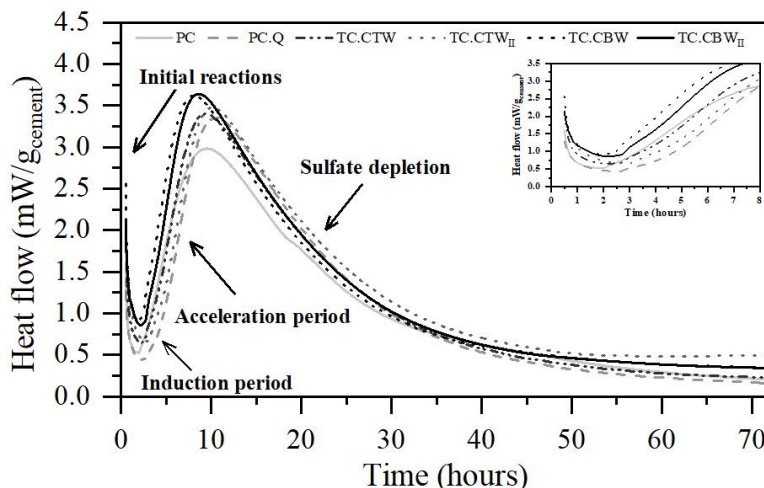
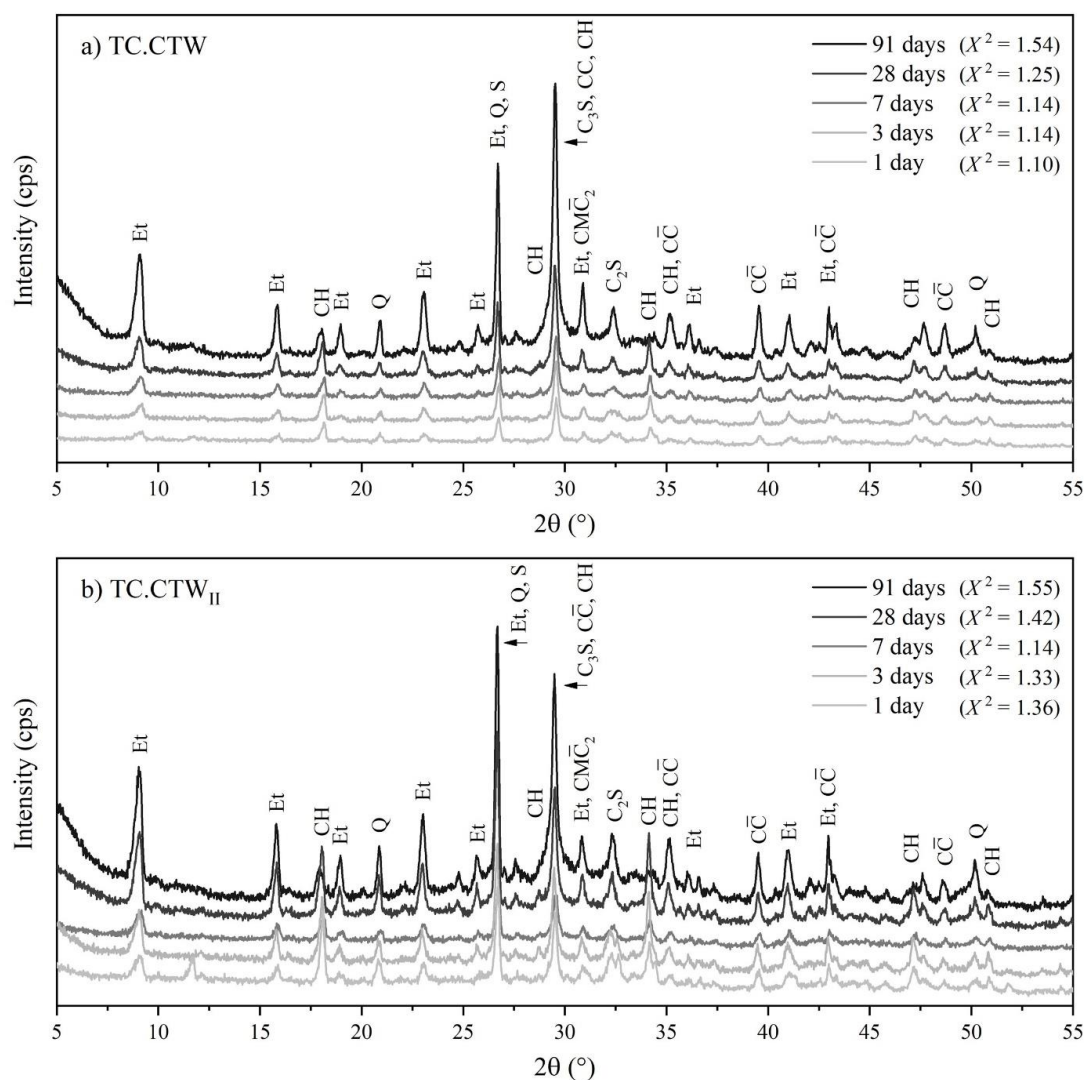




Figure 8 - (a) X-ray diffractometry of TC.CTW and (b) TC.CTW<sub>II</sub> pastes

**Note:** CH:  $\text{Ca}(\text{OH})_2$ , Et:  $\text{Ca}_6\text{Al}(\text{OH})_{12}(\text{SO}_4)_3 \cdot 26\text{H}_2\text{O}$ ,  $\text{C}_3\text{S}$ :  $\text{Ca}_3\text{SiO}_5$ ,  $\text{C}_2\text{S}$ :  $\text{Ca}_2\text{SiO}_4$ , Q:  $\text{SiO}_2$ ,  $\text{C}\bar{\text{C}}$ :  $\text{CaCO}_3$ ,  $\text{CMC}_2$ :  $\text{CaMg}(\text{CO}_3)_2$  and S:  $\text{Al}_2\text{SiO}_5$ .

The qualitative analysis of the mineralogical composition indicates that the ternary cements are made up of crystalline phases equivalent to those found in the literature on TCs containing calcined natural clays and natural calcitic limestone. In other words, the pastes contain a combination of minerals from hydration (calcium hydroxide and ettringite) and anhydrous phases remaining from the clinker (silicates, aluminates, quartz, and calcite), in addition to compounds from the inert or low reactive phases of the waste material (sillimanite, mullite, dolomite, etc.). These results indicate that, regarding the type of minerals formed during hydration up to 91 days, ternary systems containing waste raw materials present a set of phases equivalent to those observed in TCs produced with natural raw materials (SHAH *et al.*, 2018; KRISHNAN *et al.*, 2019; SHARMA *et al.*, 2021).

The quantification of the main phases of the mineralogical composition of the pastes determined by the Rietveld method is shown in Figure 10. For the PC paste, an increase in portlandite and ettringite content, as well as in non-crystalline phases, is observed. The main amorphous phase identified in pastes is C-S-H. This performance is characteristic of high initial strength cements, which present a large part of the formation of C-S-H in the first days of hydration (MEHTA; MONTEIRO, 2008).

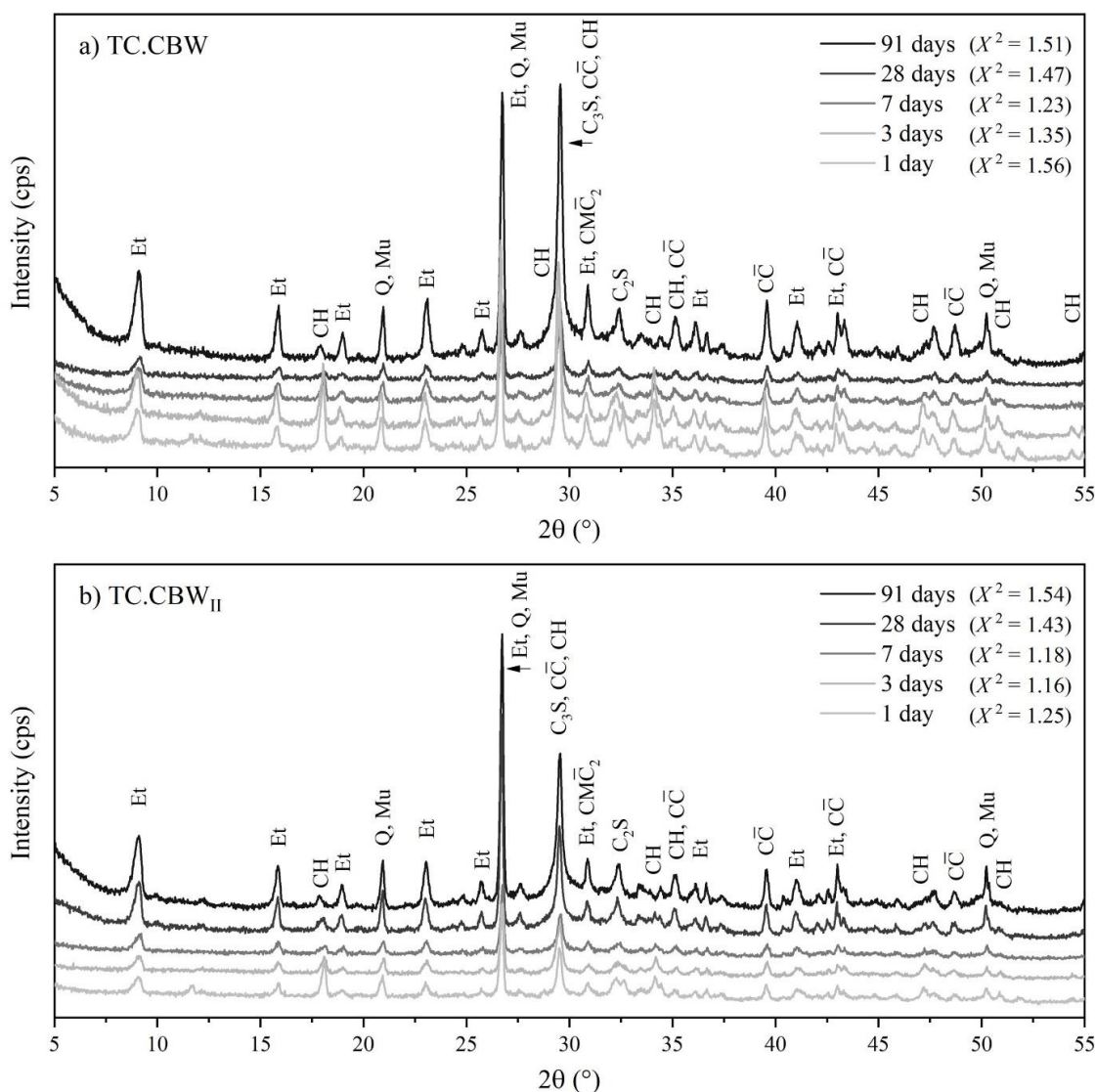
For the ternary systems, the nucleation effect, caused by the increase in the specific surface area when adding the waste, can be observed by the difference between the  $\text{Ca}(\text{OH})_2$  contents of the PC.Q paste and the respective TC after one day of hydration. Thus, positive variations are observed, indicating that both wastes accelerated the cement hydration kinetics in the initial hours, as observed in the isothermal calorimetry. The

formation of  $\text{Ca}(\text{OH})_2$  was 49% higher in TC.CTWII and 14% higher in TC.CBW, when compared to PC.Q.

The pozzolanic properties of the wastes can be verified based on the consumption of calcium hydroxide and the increase in the content of non-crystalline phases between the ages of 1 and 91 days. For all ternary systems, the  $\text{Ca}(\text{OH})_2$  consumption was above 80% and was accompanied by an increased content of non-crystalline phases. Furthermore, for both CTW and CBW, the change in the ceramic waste/CTW ratio optimised the pozzolanic reaction. Based on portlandite consumption (up to 92% reduction) and formation of amorphous phases (up to 21% increase), the CBW system was the ceramic waste with the highest pozzolanic reactivity. Variations of the same order (up to 90%) were identified in ternary cements containing calcined clays with varying contents of metakaolinite (AVET; SCRIVENER, 2018; MARAGHECHI, *et al.* 2018). The reduced reactivity of CTW, when compared to CBW, may be associated with the production temperature of the materials (up to 1200 °C and 950 °C, respectively) (OLIVEIRA.; HOTZA, 2015). When exceeding the range of dehydroxylation of clay minerals (600 and 850 °C), the thermal treatment of the clays of origin led to mineral recrystallisation and reduced pozzolanic reactivity (HOLLANDERS *et al.*, 2016; TIRONI *et al.*, 2014a).

The variation in ettringite content tends to stabilise after 7 days. This behavior is typical of ettringite formation at early ages and has been verified in ternary systems containing non-residual raw materials (KRISHNAN; EMMANUEL; BISHNOI, 2019).

Figure 9 - (a) X-ray diffractometry of TC.CBW and (b) TC.CBW<sub>II</sub> pastes



**Note:** CH:  $\text{Ca}(\text{OH})_2$ , Et:  $\text{Ca}_6\text{Al}(\text{OH})_{12}(\text{SO}_4)_3 \cdot 26\text{H}_2\text{O}$ ,  $\text{C}_3\text{S}$ :  $\text{Ca}_3\text{SiO}_5$ ,  $\text{C}_2\text{S}$ :  $\text{Ca}_2\text{SiO}_4$ , Q:  $\text{SiO}_2$ , CC:  $\text{CaCO}_3$ ,  $\text{CMC}_2$ :  $\text{CaMg}(\text{CO}_3)_2$  and Mu:  $\text{Al}_{2,41}\text{Si}_{0,59}\text{O}_{4,793}$ .

For the quartz paste (PC.Q), the portlandite content and non-crystalline phases are increasing and are in agreement with the behaviour observed in the cement paste without substitutions. The portlandite content at 28 days (4.54%) is significantly higher than that of TC.CTW (2.73%), TC.CTWII (3.88%), TC.CBW (0.93%) and TC.CBWII (0.51%), indicating a pozzolanic contribution of SCM in addition to the filler effect.

### Influence of dosage on axial compressive strength of pastes

The axial compressive strength data of the pastes are shown in Figure 11. The TC pastes performed similarly to the quartz compositions for up to 3 days. From that age onwards, the difference verified for the TC pastes shows the pozzolanic potential of the applied SCM. At 28 days, the ternary compositions reached at least 70% of the compressive strength of the PC paste. In this scenario, considering that the replacement applied was approximately 50% of the clinker, the results suggest that smaller replacements can lead to strengths equivalent to that of PC after 28 days.

Figure 10 - Main phases of the mineralogical composition of the pastes of reference cements (PC and PC.Q) and ternaries (TC) over time

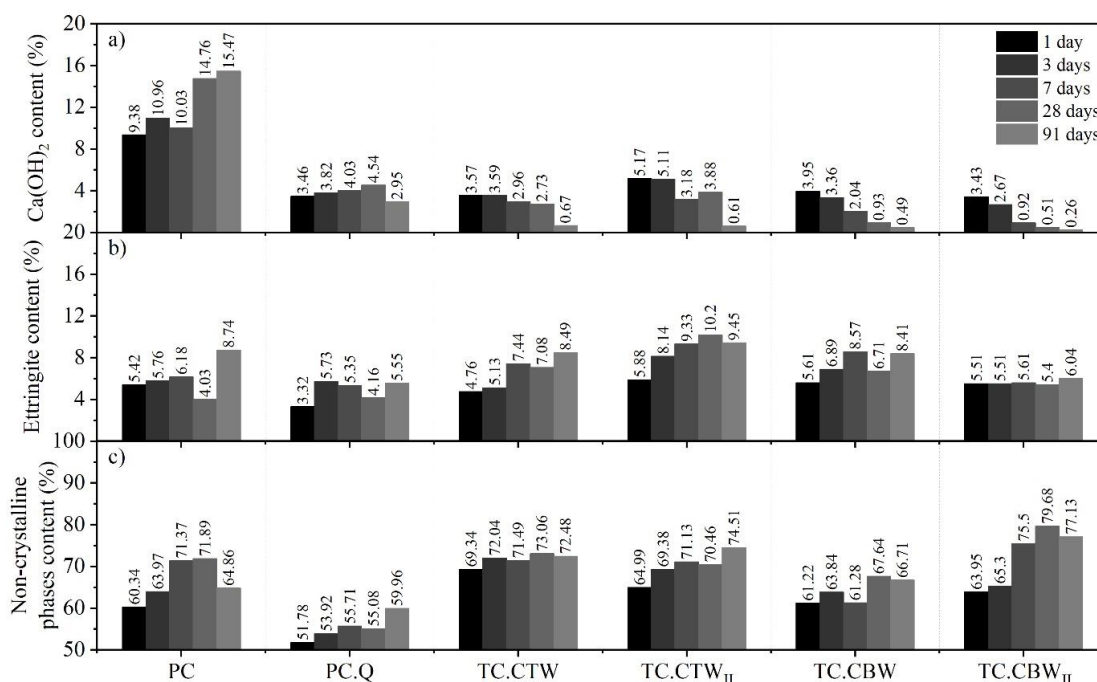
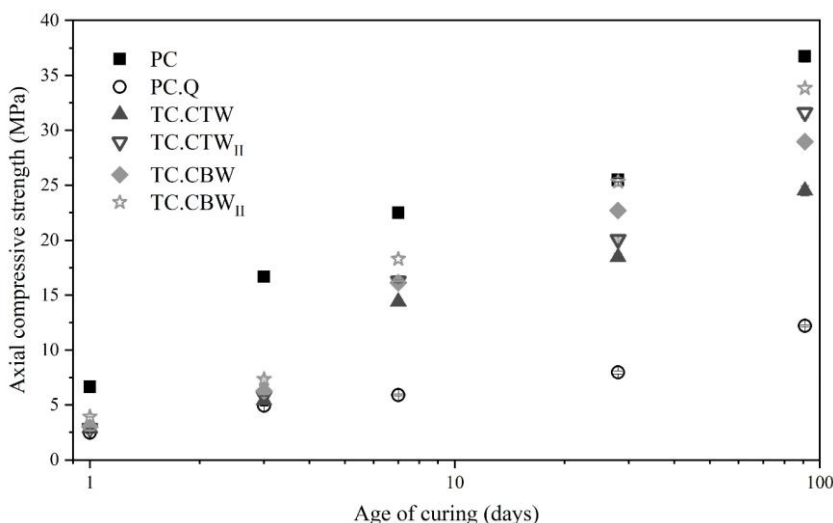


Figure 11 - Axial compressive strength of reference (PC and PC.Q) and ternary (TC) cement pastes over time



At 91 days, the CBW/MW proportion change caused about 10% higher compressive strength for TC.CBWII when compared to TC.CBW. Among ternary systems, the use of CBW led to superior compressive strength, corroborating the results of the mineralogical analysis by the Rietveld method, which indicated it as the most reactive. The axial compressive strength of the proposed TCs shows a tendency to approach the performance of the PC after 7 days. The results are compatible with the mechanical performance in the literature, which presents strengths of 20 to 40 MPa at 91 days for calcined clays with up to 30% metakaolinite (AVET *et al.*, 2016; KRISHNAN; BISHNOI, 2018).

## Conclusions

Based on the results, the following conclusions can be drawn:

- (a) the specific surface area of the raw materials is the main factor that governs the rheological performance of ternary cement pastes. An increase in this physical property implies an increase in yield stress and plastic viscosity. On the other hand, the opposite is observed for the spread diameter;
- (b) due to the high specific surface area (double the CTW area), the CBW accelerated the hydration kinetics more significantly, indicating the occurrence of the nucleation effect in the first 72 hours;
- (c) when hydrated, the ternary formulations presented crystalline phases equivalent to those verified in the literature on TCs containing calcined natural clays and natural calcitic limestone. The pastes consist of anhydrous phases and hydrated clinker products combined with compounds from the inert or less reactive phases of clay and carbonate sources;
- (d) quantitative analysis of the mineralogical composition up to 91 days indicated that CBW and CTW have pozzolanic reactivity, with consumption of up to 92% of calcium hydroxide and an increase in non-crystalline phases (including C-S-H);
- (e) CTW showed reduced reactivity compared to CBW, which was attributed to the material production temperature and the clay mineral recrystallisation process. Thus, the results suggest that clayey wastes produced at temperatures close to 850 °C are more reactive;
- (f) the TCs reached at least 70% of the axial compressive strength of the high early strength Portland cement paste at 28 days, suggesting that replacements lower than 50% can lead to strengths equivalent to the reference paste; and
- (g) regarding the analysed rheological and hydration properties, the ternary cements that incorporate waste from ceramic bricks, tiles, marble, and phosphogypsum showed similar behaviour to the systems produced with natural raw materials indicated in the literature. These results suggest that residual raw materials can be used to produce TCs. Future studies may expand the analysis of other characteristics of these cements, such as the use of other waste raw materials, interaction with chemical admixtures, and the study of the durability of the material.

## References

- ABU, M. J.; MOHAMED, J. J.; AHMAD, Z. A. Synthesis of high purity titanium silicon carbide from elemental powders using arc melting method. **International Journal of Refractory Metals and Hard Materials**, v. 47, p. 86-92, 2014.
- AKHLAGHI, O. *et al.* Modified poly (carboxylate ether)-based superplasticizer for enhanced flowability of calcined clay-limestone-gypsum blended Portland cement. **Cement and Concrete Research**, v. 101, p. 114-122, 2017.
- ALTUN, İ. A.; SERT, Y. Utilization of weathered phosphogypsum as set retarder in Portland cement. **Cement and Concrete Research**, v. 34, n. 4, p. 677-680, 2004.
- ALUJAS, A. *et al.* Pozzolanic reactivity of low grade kaolinitic clays: Influence of calcination temperature and impact of calcination products on OPC hydration. **Applied Clay Science**, v. 108, p. 94-101, 2015.
- AMERICAN SOCIETY FOR TESTING AND MATERIALS. **C 109**: standard test method for compressive strength of hydraulic cement mortars. West Conshohocken, 2016.
- AMERICAN SOCIETY FOR TESTING AND MATERIALS. **C 114-18**: standard test methods for chemical analysis of hydraulic cement. West Conshohocken, 2018.

- AMERICAN SOCIETY FOR TESTING AND MATERIALS. **C 1679**: standard practice for measuring hydration kinetics of hydraulic cementitious mixtures using isothermal calorimetry. West Conshohocken, 2017.
- AMERICAN SOCIETY FOR TESTING AND MATERIALS. **E 1269-11**: standard test method for determining specific heat capacity by differential scanning calorimetry. West Conshohocken, 2018.
- ANTONI, M. *et al.* Cement substitution by a combination of metakaolin and limestone. **Cement and Concrete Research**, v. 42, n. 12, p. 1579-1589, 2012.
- ARANDA, M. A. G.; DE LA TORRE, A. G.; LEÓN-REINA, L. Rietveld quantitative phase analysis of OPC clinkers, cements and hydration products. **Reviews in Mineralogy and Geochemistry**, v. 74, n. 1, p. 169-209, 2012.
- ASSOCIAÇÃO BRASILEIRA DE NORMAS TÉCNICAS. **NBR 16697**: cimento Portland: requisitos. Rio de Janeiro, 2018.
- ASSOCIAÇÃO BRASILEIRA DE NORMAS TÉCNICAS. **NBR 9831**: cimento Portland para poços petrolíferos: requisitos e métodos de ensaio. Rio de Janeiro, 2020.
- AVET, F. *et al.* Development of a new rapid, relevant and reliable (R<sup>3</sup>) test method to evaluate the pozzolanic reactivity of calcined kaolinitic clays. **Cement and Concrete Research**, v. 85, p. 1-11, 2016.
- AVET, F.; SCRIVENER, K. Investigation of the calcined kaolinite content on the hydration of Limestone Calcined Clay Cement (LC<sup>3</sup>). **Cement and Concrete Research**, v. 107, p. 124-135, 2018.
- BESSAIRES-BEY, H. *et al.* Organic admixtures and cement particles: Competitive adsorption and its macroscopic rheological consequences. **Cement and Concrete Research**, v. 80, p. 1-9, 2016.
- CALLIGARIS, G. A. *et al.* On the quantitative phase analysis and amorphous content of triacylglycerols materials by X-ray Rietveld method. **Chemistry and physics of lipids**, v. 212, p. 51-60, 2018.
- CLAISSE, P. A.; LORIMER, P.; OMARI, M. A. Workability of cement pastes. **ACI Materials Journal**, v. 98, n. 6, p. 476-482, 2001.
- COSTA, A. R. D. *et al.* Hydration of sustainable ternary cements containing phosphogypsum. **Sustainable Materials and Technologies**, v. 28, p. e00280, 2021.
- DHANDAPANI, Y.; SANTHANAM, M. Assessment of pore structure evolution in the limestone calcined clay cementitious system and its implications for performance. **Cement and Concrete Composites**, v. 84, p. 36-47, 2017.
- FAVIER, A. *et al.* The effect of limestone on the performance of ternary blended cement LC<sup>3</sup>: limestone, calcined clays and cement. In: **CALCINED Clays for Sustainable Concrete**. Dordrecht: Springer, 2018.
- FERREIRO, S.; HERFORT, D.; DAMTOFT, J. S. Influence of clay type on performance of calcined clay–Limestone Portland cements. In: **Calcined Clays for Sustainable Concrete**. Dordrecht: Springer, 2018.
- HAQUE, M. A. *et al.* Improvement of physico-mechanical and microstructural properties of magnesium phosphate cement composites comprising with Phosphogypsum. **Journal of Cleaner Production**, v. 261, p. 121268, 2020.
- HOLLANDERS, S. *et al.* Pozzolanic reactivity of pure calcined clays. **Applied Clay Science**, v. 132, p. 552-560, 2016.
- KRISHNAN, S. *et al.* Industrial production of limestone calcined clay cement: experience and insights. **Green Materials**, v. 7, n. 1, p. 15-27, 2019.
- KRISHNAN, S.; BISHNOI, S. Understanding the hydration of dolomite in cementitious systems with reactive aluminosilicates such as calcined clay. **Cement and Concrete Research**, v. 108, p. 116-128, 2018.
- KRISHNAN, S.; EMMANUEL, A. C.; BISHNOI, S. Hydration and phase assemblage of ternary cements with calcined clay and limestone. **Construction and Building Materials**, v. 222, p. 64-72, 2019.
- LI, H. *et al.* Effect of fatty acid methyl ester polyoxyethylene ether on the rheological properties of cement filled with artificial marble waste powders. **Journal of Cleaner Production**, v. 328, p. 129503, 2021.
- LONG, W. J. *et al.* Printability and particle packing of 3D-printable limestone calcined clay cement composites. **Construction and Building Materials**, v. 282, p. 122647, 2021.
- MADSEN, I. C.; SCARLETT, N. V. Y.; KERN, A. Description and survey of methodologies for the determination of amorphous content via X-ray powder diffraction. **Zeitschrift für Kristallographie**, v. 226,

n. 12, p. 944-955, 2011.

MANTELLATO, S.; PALACIOS, M.; FLATT, R. J. Reliable specific surface area measurements on anhydrous cements. **Cement and Concrete Research**, v. 67, p. 286-291, 2015.

MARAGHECHI, H. *et al.* Performance of Limestone Calcined Clay Cement (LC<sup>3</sup>) with various kaolinite contents with respect to chloride transport. **Materials and Structures**, v. 51, n. 5, p. 1-17, 2018.

MEHDIPOUR, I.; KHAYAT, K. H. Effect of particle-size distribution and specific surface area of different binder systems on packing density and flow characteristics of cement paste. **Cement and Concrete Composites**, v. 78, p. 120-131, 2017.

MEHTA, P. K.; MONTEIRO, P. J. **Concrete: microestrutura, propriedades e materiais**. 3. ed. São Paulo: Pini, 2008.

MITTEMEIJER, E. J.; SCARDI, P. (ed.). **Diffraction analysis of the microstructure of materials**. Heidelberg: Springer Science & Business Media, 2004.

NAIR, N. *et al.* A study on fresh properties of limestone calcined clay blended cementitious systems. **Construction and Building Materials**, v. 254, p. 119326, 2020.

OLIVEIRA, A. P. N.; HOTZA, D. **Tecnologia de Fabricação de revestimentos cerâmicos**. Editora UFSC, Ed. 2. Florianópolis, 2015.

PEREZ, A. *et al.* Influence of the Manufacturing Process on the Performance of Low Clinker, Calcined Clay-Limestone Portland Cement. In: **Calcined Clays for Sustainable Concrete**. Springer, Dordrecht, p. 283-289, 2015.

PUERTA-FALLA, G. *et al.* Elucidating the role of the aluminous source on limestone reactivity in cementitious materials. **Journal of the American Ceramic Society**, v. 98, n. 12, p. 4076-4089, 2015.

RAMACHANDRAN, V. S. *et al.* **Handbook of thermal analysis of construction materials**. New York: Noyes Publications, William Andrew Publishing, 2002.

RASHAD, A. M. Phosphogypsum as a construction material. **Journal of Cleaner Production**, v. 166, p. 732-743, 2017.

ROSALES, J. *et al.* Treated phosphogypsum as an alternative set regulator and mineral addition in cement production. **Journal of Cleaner Production**, v. 244, p. 118752, 2020.

SABIR, B. B.; WILD, S.; BAI, J. Metakaolin and calcined clays as pozzolans for concrete: a review. **Cement and Concrete Composites**, v. 23, n. 6, p. 441-454, 2001.

SHAH, V. *et al.* Changes in microstructure characteristics of cement paste on carbonation. **Cement and Concrete Research**, v. 109, p. 184-197, 2018.

SHARMA, M. *et al.* Limestone calcined clay cement and concrete: a state-of-the-art review. **Cement and Concrete Research**, v. 149, p. 106564, 2021.

TIRONI, A. *et al.* Kaolinitic calcined clays: Portland cement system: hydration and properties. **Construction and Building Materials**, v. 64, p. 215-221, 2014a.

TIRONI, A. *et al.* Thermal analysis to assess pozzolanic activity of calcined kaolinitic clays. **Journal of Thermal Analysis and Calorimetry**, v. 117, n. 2, p. 547-556, 2014b.

TIRONI, A.; SCIAN, A. N.; IRASSAR, E. F. Blended cements with limestone filler and kaolinitic calcined clay: Filler and pozzolanic effects. **Journal of Materials in Civil Engineering**, v. 29, n. 9, p. 04017116, 2017.

TOBY, B. H.; VON DREELE, R. B. GSAS-II: the genesis of a modern open-source all purpose crystallography software package. **Journal of Applied Crystallography**, v. 46, n. 2, p. 544-549, 2013.

ZHANG, L. *et al.* Effect of polycarboxylate ether comb-type polymer on viscosity and interfacial properties of kaolinite clay suspensions. **Journal of Colloid and Interface Science**, v. 378, n. 1, p. 222-231, 2012.

**Ana Rita Damasceno Costa**

Programa de Pós-Graduação em Engenharia Civil, Escola Politécnica | Universidade Federal da Bahia | Rua Professor Aristides Novis, 02, Federação | Salvador - BA - Brasil | CEP 40210-630 | E-mail: rita.damasceno@ufba.br

**Jardel Pereira Gonçalves**

Centro Interdisciplinar de Energia e Ambiente, Escola Politécnica | Universidade Federal da Bahia | Tel.: (71) 3283 9485 | E-mail: jardelpg@ufba.br

***Ambiente Construído***

Revista da Associação Nacional de Tecnologia do Ambiente Construído

Av. Osvaldo Aranha, 99 - 3º andar, Centro

Porto Alegre - RS - Brasil

CEP 90035-190

Telefone: +55 (51) 3308-4084

[www.seer.ufrgs.br/ambienteconstruido](http://www.seer.ufrgs.br/ambienteconstruido)

[www.scielo.br/ac](http://www.scielo.br/ac)

E-mail: [ambienteconstruido@ufrgs.br](mailto:ambienteconstruido@ufrgs.br)



This is an open-access article distributed under the terms of the Creative Commons Attribution License.